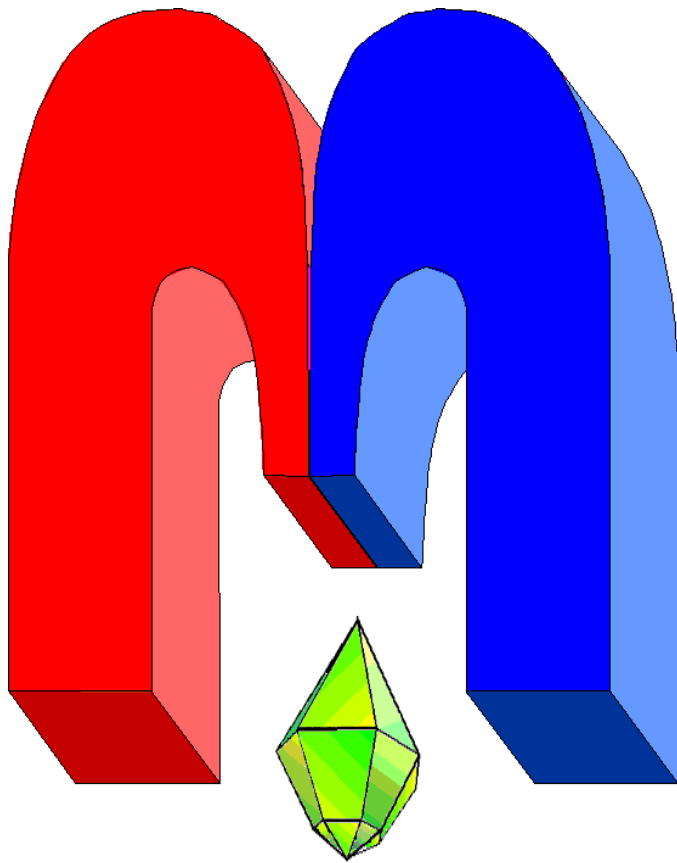


ISSN 2072-5981
doi: 10.26907/mrsej



***magnetic
Resonance
in Solids***

Electronic Journal

Volume 21

Issue 5

Paper No 19503

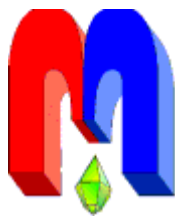
1-8 pages

2019

doi: 10.26907/mrsej-19503

<http://mrsej.kpfu.ru>

<http://mrsej.ksu.ru>



Established and published by Kazan University
Endorsed by International Society of Magnetic Resonance (ISMAR)
Registered by Russian Federation Committee on Press (#015140),
August 2, 1996
First Issue appeared on July 25, 1997

© Kazan Federal University (KFU)*

"Magnetic Resonance in Solids. Electronic Journal" (MRSej) is a peer-reviewed, all electronic journal, publishing articles which meet the highest standards of scientific quality in the field of basic research of a magnetic resonance in solids and related phenomena.

Indexed and abstracted by
Web of Science (ESCI, Clarivate Analytics, from 2015), Scopus (Elsevier, from 2012), RusIndexSC (eLibrary, from 2006), Google Scholar, DOAJ, ROAD, CyberLeninka (from 2006), SCImago Journal & Country Rank, etc.

Editor-in-Chief

Boris Kochelaev (KFU, Kazan)

Honorary Editors

Jean Jeener (Universite Libre de Bruxelles, Brussels)

Raymond Orbach (University of California, Riverside)

Executive Editor

Yurii Proshin (KFU, Kazan)
mrsej@kpfu.ru



This work is licensed under a [Creative Commons Attribution-ShareAlike 4.0 International License](https://creativecommons.org/licenses/by-sa/4.0/).



This is an open access journal which means that all content is freely available without charge to the user or his/her institution. This is in accordance with the [BOAI definition of open access](https://www.boai.ru/).

Technical Editor

Maxim Avdeev (KFU, Kazan)

Editors

Vadim Atsarkin (Institute of Radio Engineering and Electronics, Moscow)

Yurij Bunkov (CNRS, Grenoble)

Mikhail Eremin (KFU, Kazan)

David Fushman (University of Maryland, College Park)

Hugo Keller (University of Zürich, Zürich)

Yoshio Kitaoka (Osaka University, Osaka)

Boris Malkin (KFU, Kazan)

Alexander Shengelaya (Tbilisi State University, Tbilisi)

Jörg Sichelschmidt (Max Planck Institute for Chemical Physics of Solids, Dresden)

Haruhiko Suzuki (Kanazawa University, Kanazawa)

Murat Tagirov (KFU, Kazan)

Dmitrii Tayurskii (KFU, Kazan)

Valentine Zhikharev (KNRTU, Kazan)

* In Kazan University the Electron Paramagnetic Resonance (EPR) was discovered by Zavoisky E.K. in 1944.

Ultrafast magnetization dynamics in thin films of $L1_0$ -ordered FePt and FePd compounds: Promising differences

A.V. Petrov¹, M.V. Pasyukov¹, R.V. Yusupov^{1,*}, S.I. Nikitin¹, A.I. Gumarov¹,
I.V. Yanilkin¹, A.G. Kiiamov¹, L.R. Tagirov^{1,2}

¹Kazan Federal University, Kremlevskaya 18, 420008 Kazan, Russia

²Zavoisky Physical-Technical Institute, FRC “Kazan Scientific Center of RAS”,
Sibirsky Trakt 10/7, 420029 Kazan, Russia

**E-mail: Roman.Yusupov@kpfu.ru*

(Received August 16, 2019; accepted August 21, 2019; published August 22, 2019)

In the paper we report on the synthesis, structural and magnetic characterization and time-resolved polar magneto-optical Kerr effect studies of thin epitaxial films of the ordered $L1_0$ -phase of FePt and FePd compounds. Time scales of the photoinduced demagnetization and magnetization recovery are found. It is shown that demagnetization of FePt and FePd films occurs on different time scales, ~ 0.2 ps and ~ 3 ps, respectively. This difference makes these films promising for artificial multilayer ferrimagnets with high perpendicular anisotropy suitable for all-optical fast high-capacity information storage devices.

PACS: 75.40.Gb, 75.47.Np, 74.25.Nf, 74.70.Ad

Keywords: palladium-iron alloy, platinum-iron alloy, epitaxial film, time-resolved magneto-optical Kerr effect, perpendicular anisotropy

1. Introduction

Rapid development of the information society is accompanied by drastic increase in data production. This development requires an increase in the capacity and data exchange rate of the information storage devices. The main type of these devices in modern data centers is the hard disc drive (HDD) based on magnetic recording media. A straightforward way to increase the hard disk capacity is to increase the recording density or, equivalently, reduce the size of the magnetic grain carrying a bit of information. However, a decrease of the magnetized grain volume is associated with the risk of a so-called superparamagnetic effect, when the particle magnetization direction becomes thermally unstable. The criterion that needs to be satisfied to ensure the stability required in data storage devices, is expressed as $K_u V / k_B T \geq 60$ [1], where K_u is the magnetic anisotropy constant, V is the particle volume, k_B is the Boltzmann constant and T is temperature. Therefore, to reduce the bit size, it is necessary to use materials with high magnetic anisotropy. It is preferable also to employ the easy-axis materials with “perpendicular” anisotropy.

In this regard, ferromagnetic thin films of the ordered $L1_0$ -phase of FePt and FePd compounds attract the attention of hard disc developers. Magnetocrystalline anisotropy constant of the $L1_0$ -FePt and $L1_0$ -FePd epitaxial films on MgO (001) substrate is of the order of 10^7 erg/cm³ [2, 3]. These films are easy-axis systems with an equilibrium direction of magnetization perpendicular to the film plane. Large value of the anisotropy constant, on one hand, allows to reduce the size of the magnetic grain staying far from the superparamagnetic limit. On the other hand, an increased value of the anisotropy constant requires sometimes unrealistic for existing writing heads of HDDs magnetic fields necessary for switching the magnetization. To reduce the switching field, the technology of heat assisted magnetic recording (HAMR) was proposed that supposes heating up of the recording medium spot by short laser pulses prior to the application of a magnetic field [4]. However, having implemented the possibility of information recording on

such media and, accordingly, having increased the capacity of hard disks many times, one will need to overcome another limitation, namely, the low speed of data exchange, especially in the recording process.

If we consider the speed of hard disc drives, then the reduction in the cycle duration for recording a bit of information is limited by the rate of increasing the magnetic field created by the recording head. As a solution that provides a way to overcome such a limitation, the possibility of switching the magnetization of materials by short intense light pulses is being actively studied. The possibility of such control was demonstrated on thin films of ferrimagnetic materials: alloys with rare-earth elements GdCoFe [5–8], TbCo [9], FeTb [10] and multilayer structures of transition metals Co/Pt [11, 12]. Also the works on the magnetization reversal of the FePtAgC [12] and FePt [13] nanoparticles prepared for HAMR are worth noting. The key point in this process is the effective amount of light pulses necessary for the magnetization reversal and saturation. In most of the works, such an amount was either not determined, or up to hundreds of pulses were required. Among the works listed above, only those devoted to the GdCoFe films reported the magnetization reversal by a single light pulse [8]. The efficiency of such magnetization switching is due, firstly, to ferrimagnetic ordering and, secondly, to the difference in the demagnetization rates of the magnetic sublattices of the material after exposure to a light pulse [8, 14, 15].

In view of the foregoing, the idea of creating a material which is simultaneously characterized by strong magnetocrystalline anisotropy allowing to increase disc capacity and ability of magnetization reversal by light pulses becomes very attractive. In this paper, we study the suitability of thin films of the ordered $L1_0$ -phase of FePt and FePd compounds for creating such magnetic medium with respect to the photo-induced magnetization dynamics in them.

2. Sample synthesis, characterization and experimental details

Thin continuous films of the ordered $L1_0$ -phase of FePd and FePt compounds were deposited by co-evaporation from high-temperature effusion cells in ultrahigh vacuum setup (SPECS, Germany). To achieve a continuous morphology of the films, the following steps were undertaken. First, a seed layer of chromium with a thickness of 3 nm was grown on MgO (001) substrates (MTI Corp., USA) held at a temperature of 600°C. This layer provides a conformal continuous coating with high adhesion to the substrate material. Then, the temperature of the substrates was lowered to the ambient one and either FePd or FePt layers with the thickness of 10 nm were deposited. After that, the films were annealed in high vacuum for 30 minutes at 650°C to promote the ordering into the $L1_0$ -phase.

Figure 1 (a) and (b), shows the low energy electron diffraction (LEED) patterns measured *in situ* on the MgO (001) substrate after its annealing in high-vacuum chamber at 800°C for 20 minutes and from the FePd film deposited onto a chromium underlayer, respectively. LEED pattern from the FePt film looks identical to Fig. 1 (b). High contrast of the patterns in both panels indicates good epitaxy and coherent cube-on-cube growth of the films on the MgO substrate.

Figure 1 (c) shows X-ray diffraction patterns of the FePt and FePd samples. Diffractograms were measured in the Bragg-Brentano geometry with Bruker D8 Advance diffractometer equipped with the Cu- K_α source (wavelength $\lambda = 1.5418 \text{ \AA}$). For FePt and FePd samples, in addition to the most intense sharp (002) diffraction maximum of the MgO substrate at $2\theta = 42.86$ degrees, relatively wide peaks are observed at 2θ values of 24.06 and 24.24 degrees corresponding to the (001) maximum, and 49.26 and 49.58 degrees corresponding to the (002) one, respectively. Positions of the maxima correspond to interplanar distances of 3.710 Å for FePt and 3.670 Å for FePd,

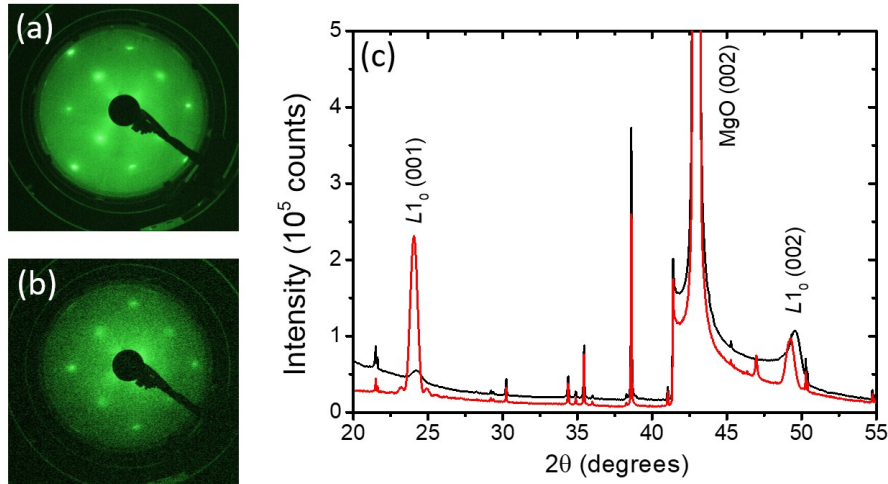


Figure 1. Low-energy electron diffraction patterns taken from the intact MgO (001) substrate (a) and from deposited PdFe film after its annealing at 650°C in vacuum (b); the electrons energy is 140 eV. X-ray diffraction patterns from the $L1_0$ -ordered FePt (red line) and FePd (black line) films on the (001)-oriented MgO (c).

close to the known values of the lattice constant c in the bulk of 3.702 Å [16] and 3.715 Å [17], respectively, for the tetragonal $L1_0$ -phase of these compounds. Lattice constant a values are 3.842 Å and 3.850 Å for the bulk $L1_0$ -FePt and FePd, respectively [16, 17]. The very fact of observing the (001) peak for both films is a qualitative signature of the tetragonal symmetry of the synthesized films; its intensity in the disordered cubic-symmetry A1-phase is zero. Thus, the grown films are single crystalline with the c -axis perpendicular to the film plane. Large width of the diffraction maxima of the films is due to the small, ~ 10 nm, film thickness [18]. Also, the intensity ratio of the (001) and (002) peaks for the FePt and FePd films are in a reasonable agreement with the calculated ones obtained with the use of the PowderCell software [19] 1.8 : 1 and 1 : 1.6, respectively. The collected structural data indicate high crystal quality and perfect epitaxy of the studied films.

Magnetic hysteresis curves of the samples were measured with vibrating sample magnetometry (VSM) option of the PPMS-9 system by Quantum Design. The field was applied perpendicular to the film plane. The results of these measurements performed at room temperature are presented in Fig. 2. Near-rectangular shapes of the hysteresis loops indicate high homogeneity and quality of the films, as well as their perpendicular anisotropy in the bulk of the film volume. The obtained coercive field values are ~ 30 mT for FePd, and ~ 110 mT for FePt; the magnetizations saturate in this configuration at ~ 0.1 T for the FePd sample and at ~ 0.5 T for the FePt.

Figure 2 shows also the quasi-equilibrium hysteresis curves obtained by the polar magneto-optical Kerr effect (MOKE) measurements at the wavelength of 800 nm. Saturation values of the Kerr angle were ~ 3 mrad for the FePd film and ~ 42 mrad for the FePt sample; note here more than an order of magnitude difference in the saturated Kerr angle for the two compounds. The shape of the MOKE hysteresis curves is almost identical to that of the static magnetization. Small discrepancies in the shapes of the curves in our opinion can be associated, first, with different rates of the magnetic field variation in the two kinds of the experiments. Another possible reason might be related to the film inhomogeneity: in magnetization measurements the result is an average over the 2×2 mm² sample area while in MOKE the beam diameter at the surface was ~ 50 μ m.

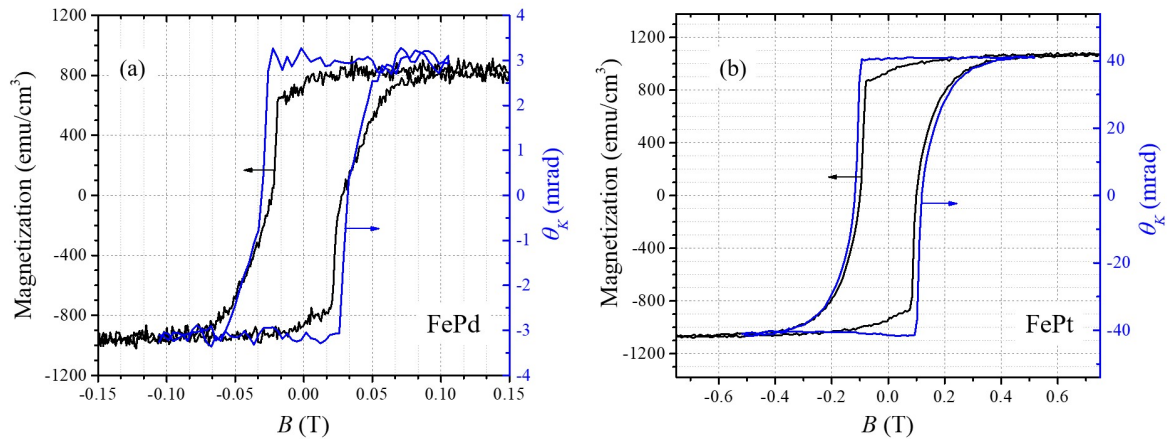


Figure 2. Dependences of the magnetization (black lines) and the equilibrium Kerr rotation angle (blue lines) on the applied magnetic field for $L1_0$ -FePd (a) and FePt (b) thin films with the field applied perpendicular to the film plane; $T = 300$ K.

Experiments on the femtosecond laser spectroscopy were performed utilizing the pump-probe scheme. In this case, a femtosecond laser system based on the Legend-USP regenerative amplifier by Coherent, Inc. (USA) was used. The laser emits light pulses with a duration of 35 fs, a central wavelength of 800 nm and a pulse repetition rate of 970 Hz. Pump light wavelength was 400 nm (second harmonic), and that of the probe was 800 nm. For the second harmonic generation, the nonlinear 140- μ m thick BBO crystal was used. The pump and probe beams were focused at the sample surface into the spots with the diameters of ~ 0.5 mm and ~ 0.2 mm with the incidence angles of 50 and 60 degrees, respectively. The pump fluence was varied in the range of 10 – 40 mJ/cm², and the probe fluence was ~ 50 μ J/cm². Magnetic field was produced by a resistive electromagnet and could be varied within ± 0.6 T range.

Magnetization dynamics was measured via the deviation of the polarization plane angle of the probe light from the equilibrium as a function of time delay between the pump and the probe. To measure the Kerr rotation angle, the probe light reflected from the sample passed through the Wollaston prism that splits the light into two orthogonally-polarized components. The intensities of these two components were detected by silicon photodiodes (Hamamatsu S2386-5K). The difference signal from the photodiode output was used to determine the deviation of the Kerr rotation angle from the equilibrium value, while the sum signal was used to measure the dynamics of the reflectivity.

3. Experimental results and discussion

We start this section with description of the procedure for extracting the time-resolved Kerr rotation angle related to the magnetization dynamics from the integral rotation angle. The last in general case has two origins: modification of the magnetization of the sample following the pump pulse and the photoinduced anisotropy not related to the magnetization. Then, a total response can be expressed as:

$$\Delta\theta(\Delta t, B) = \Delta\theta_K(\Delta t, B) + \Delta\theta_{an}(\Delta t), \quad (1)$$

where the first term on the right side, $\Delta\theta_K$ is the Kerr rotation angle and the second term, $\Delta\theta_{an}$ corresponds to the polarization plane angle rotation due to photoinduced anisotropy. To separate these contributions, the dependence of the total rotation angle $\Delta\theta$ on the time delay Δt should

be measured at two applied magnetic fields of equal magnitudes and opposite directions, $+B$ and $-B$. The magnetic contribution then corresponds to the odd with respect to the magnetic field component (half-difference of the two responses), and the nonmagnetic contribution corresponds to the even component (their half-sum):

$$\Delta\theta_K(\Delta t, B) = \frac{\Delta\theta(\Delta t, +B) - \Delta\theta(\Delta t, -B)}{2}, \quad (2)$$

$$\Delta\theta_{\text{an}}(\Delta t, B) = \frac{\Delta\theta(\Delta t, +B) + \Delta\theta(\Delta t, -B)}{2}. \quad (3)$$

Results of the procedures described above are shown in Fig. 3. The measurements were performed at a pump fluence of 40 mJ/cm^2 at room temperature. It can be seen that for both the FePt and FePd films the nonmagnetic contribution to the rotation angle prevails over the magnetic one. For the FePd film the difference in the magnetic and non-magnetic contributions is more pronounced, in our opinion, due to a lower value of the equilibrium saturated Kerr angle (Fig. 2).

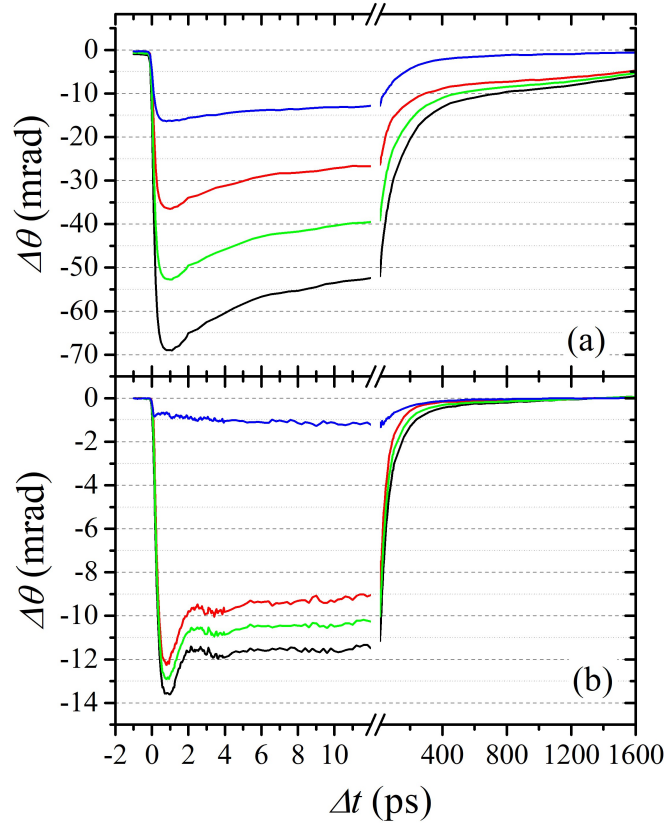


Figure 3. Dependences of the total polarization plane rotation angle $\Delta\theta$ of the probe beam on the time delay Δt between the pump and the probe pulses measured with the magnetic field values of -0.5 T (black line) and $+0.5 \text{ T}$ (red line) for $L1_0$ -ordered FePt (a) and FePd (b) thin films on the (001)-MgO substrate; the pump fluence $\Phi = 40 \text{ mJ/cm}^2$. Kerr rotation angle and photoinduced anisotropy signals extracted using Eqs. (2) and (3) are shown by the blue and the green lines, respectively.

In the case of the FePt film, the pump pulse leads to the suppression of the magnetization which occurs on a time scale of $\sim 0.2 \text{ ps}$. This is followed by a smooth transition to the magnetization recovery. The recovery of magnetization of the FePt sample can be described by the sum of two exponential decays with characteristic times of $\sim 15 \text{ ps}$ and $\sim 180 \text{ ps}$.

The dynamics of the Kerr rotation angle for the FePd film is significantly different. First, within ~ 0.1 ps, an almost instantaneous demagnetization step is observed, which is followed by a slower magnetization suppression that develops on a scale of ~ 3 ps and reaches a maximum at ~ 20 ps. The subsequent relaxation process can be described by a decaying exponent with a characteristic time of ~ 150 ps. Notably different demagnetization dynamics has been reported recently for PdFe thin film [23]: it is almost identical to that observed for FePt, both qualitatively and quantitatively. On the other hand, the dynamics for our FePt film reproduces well the results of Ref. [23]. Once the measurement technique is developed and tested it makes sense to perform a comparative study of FePd films prepared utilizing the co-evaporation and multilayer technologies. This in turn could reveal a possibility of the demagnetization dynamics tuning by means of the synthesis procedure adjustment.

As far as dependence of the magnetization dynamics on the pump fluence is concerned, MOKE transients of both the FePt and FePd $L1_0$ -ordered films grow in magnitude with fluence increase and do not reveal saturation within the range of $20 - 40$ mJ/cm² (Fig. 4). The response character in this range remains qualitatively identical for each compound. With a fluence value of 40 mJ/cm², the maximum magnetization suppression for both FePt and FePd films reaches the value of $\sim 40\%$ (Fig. 4, scale on the right).

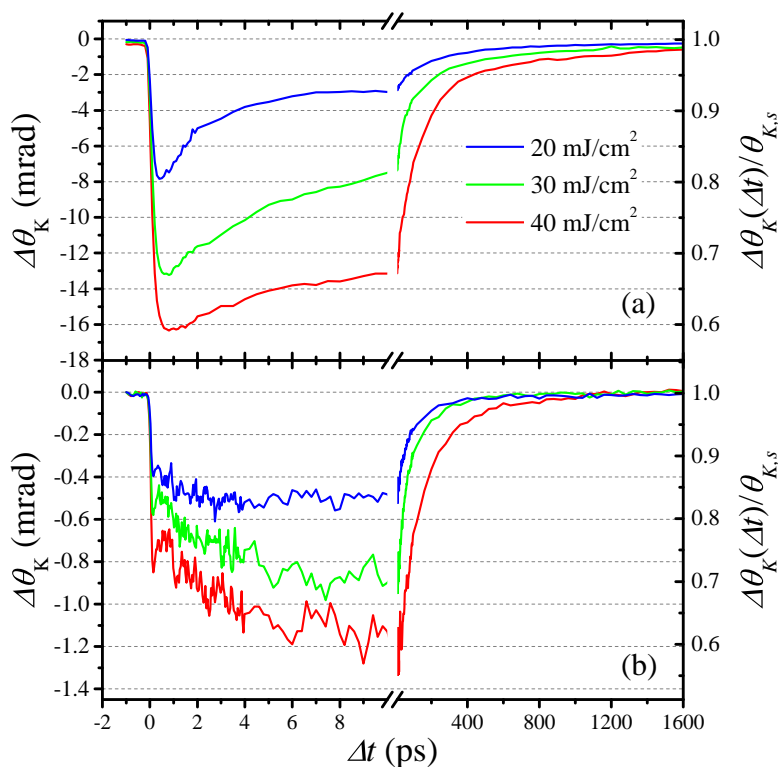


Figure 4. Variation with the pump fluence of the ultrafast magnetization dynamics in $L1_0$ -ordered FePt (a) and FePd (b) films after the pulsed photoexcitation. The pump fluence values are 20 mJ/cm² (blue lines), 30 mJ/cm² (green) and 40 mJ/cm² (red); $T = 300$ K. The scale on the right side of the panels serves for an estimate of the degree of demagnetization.

The discovered differences in ultrafast magnetization dynamics of the $L1_0$ -ordered FePt and FePd epitaxial thin films after the pulsed photoexcitation open a gateway of producing the artificial ferrimagnets suitable for all-optical magnetization reversal. Indeed, in Refs. [8, 14, 15] the conditions necessary for the photoinduced magnetization reversal in ferrimagnetic GdFeCo al-

loys by ultrashort light pulse were discussed. The authors put forward the idea that a significant difference in demagnetization rates of sublattices of the ferrimagnet is needed. It should be noted that the demagnetization of a pure iron film occurs in one step on a time scale of ~ 1 ps [20–22], with the subsequent partial recovery with a rate characteristic for the electron-lattice relaxation. Demagnetization of a pure Gd film proceeds in two stages: a fast, occurring on a scale of ~ 1 ps and a slow, lasting up to ~ 100 ps [24,25]. In the ferrimagnetic material, even taking into account the exchange interaction, the sublattices of these elements demagnetize at different rates.

In these conditions, the sequence of the events looks as follows [8]. The system starts from the equilibrium supposing non-zero spontaneous magnetization of each sublattice and their antiparallel alignment. After a pulsed photoexcitation, magnetic order melts in the CoFe sublattice in less than a picosecond, with the Gd sublattice being just slightly perturbed. At the next stage, CoFe-sublattice starts to cool down and recover magnetic ordering in the magnetic field created by the demagnetizing Gd-sublattice; at this stage, magnetization of the CoFe-sublattice is aligned parallel to that of the Gd one. After about 100 ps, the magnetization of the Gd-sublattice gets melted while that of the CoFe-one recovers. After that, the Gd-moment ensemble starts to cool down, and after few hundreds of picoseconds, the system finds itself in a ferrimagnetic state with the magnetizations of the sublattices inverted with respect to the initial configuration.

The $L1_0$ -ordered FePd and FePt films studied in the present work reveal the difference in the temporal evolution of the magnetization that are qualitatively similar to those observed for sublattices of the ferrimagnetic GdCoFe films. In this case, it looks promising to combine these two films into an exchange-coupled heterostructure comprising artificial ferrimagnetic material with high perpendicular magnetic anisotropy. A possibility of fabrication of artificial multilayer-based ferrimagnets with perpendicular anisotropy has been shown, *e.g.*, in Ref. [11]. High anisotropy will ensure high-density of the information storage while the difference in demagnetization rates would provide an ability of ultrafast photoinduced magnetization reversal.

Acknowledgments

The work was supported by the Russian Scientific Foundation, project No. 18-12-00459. R.V.Yu. acknowledges the partial support from the subsidy allocated to Kazan Federal University to fulfill the state assignment in the sphere of scientific activities (task No. 3.7704.2017/6.7). L.R.T. acknowledges the partial support by the state assignment No. AAAA-A18-118030690040-8.

References

1. Weller D., Moser A. *IEEE Trans. Magn.*, **35** 4423 (1999)
2. Ivanov O. A., Solina L. V., Demshina V. A. *Phys. Met. Metallogr.* **35**, 81 (1973)
3. Miyata N., Asami H., Mizushima T., Sato K. *J. Phys. Soc. Jpn.* **59**, 1817 (1990)
4. Kryder M. H., Gage E. C., McDaniel T. W., Challener W. A., Rottmayer R. E., Ju G., Hsia Y. T., Erden M. F. *Proc. IEEE* **96**, 1810 (2008)
5. Stanciu C. D., Hansteen F., Kimel A. V., Kirilyuk A., Tsukamoto A., Itoh A., Rasing T. *Phys. Rev. Lett.* **99**, 047601 (2007)
6. Vahaplar K., Kalashnikova A. M., Kimel A. V., Hinzke D., Nowak U., Chantrell R., Tsukamoto A., Itoh A., Kirilyuk A., Rasing T. *Phys. Rev. Lett.* **103**, 117201 (2009)
7. Radu I., Vahaplar K., Stamm C., Kachel T., Pontius N., Dürr H. A., Ostler T. A., Barker J., Evans R. F. L., Chantrell R. W., Tsukamoto A. *Nature* **472**, 205 (2011)
8. Ostler T. A., Barker J., Evans R. F. L., Chantrell R. W., Atxitia U., Chubykalo-Fesenko O., El Moussaoui S., Le Guyader L. B. P. J., Mengotti E., Heyderman L. J., Nolting F. *Nat. Commun.* **3**, 666 (2012)

9. Alebrand S., Gottwald M., Hehn M., Steil D., Cinchetti M., Lacour D., Fullerton E. E., Aeschlimann M., Mangin S. *Appl. Phys. Lett.* **101**, 162408 (2012)
10. Hassdenteufel A., Hebler B., Schubert C., Liebig A., Teich M., Helm M., Aeschlimann M., Albrecht M., Bratschitsch R. *Adv. Mater.* **25**, 3122 (2013)
11. Mangin S., Gottwald M., Lambert C. H., Steil D., Uhlř V., Pang L., Hehn M., Alebrand S., Cinchetti M., Malinowski G., Fainman Y. *Nat. Mater.* **13**, 286 (2014)
12. Lambert C. H., Mangin S., Varaprasad B. C. S., Takahashi Y. K., Hehn M., Cinchetti M., Malinowski G., Hono K., Fainman Y., Aeschlimann M., Fullerton E. E. *Science* **345**, 1337 (2014)
13. John R., Berritta M., Hinzke D., Müller C., Santos T., Ulrichs H., Nieves P., Walowski J., Mondal R., Chubykalo-Fesenko O., McCord J. *Sci. Rep.* **7**, 4114 (2017)
14. Mentink J. H., Hellsvik J., Afanasiev D. V., Ivanov B. A., Kirilyuk A., Kimel A. V., Eriksson O., Katsnelson M. I., Rasing T. *Phys. Rev. Lett.* **108**, 057202 (2012)
15. Graves C. E., Reid A. H., Wang T., Wu B., De Jong S., Vahaplar K., Radu I., Bernstein D. P., Messerschmidt M., Müller L., Coffee R. *Nat. Mater.* **12**, 293 (2013)
16. Menshikov A., Tarnóczy T., Krén E. *Phys. Status Solidi A* **28**, K85 (1975)
17. Pal'guyev Y. V., Kuranov A. A., Syukin P. N., Didorenko F. A. *Phys. Met. Metallogr.* **42**, 46 (1976)
18. Patterson A. *Phys. Rev.* **56**, 978 (1939)
19. Kraus W., Nolze G. *J. Appl. Cryst.* **29**, 303 (1996)
20. Weber A., Pressacco F., Guenther S., Mancini E., Oppeneer P. M., Back C. H. *Phys. Rev. B.* **84**, 132412 (2011)
21. Koopmans B., Malinowski G., Dalla Longa F., Steiauf D., Fähnle M., Roth T., Cinchetti M., Aeschlimann M. *Nat. Mater.* **9**, 259 (2010)
22. Carpena E., Mancini E., Dallera C., Brenna M., Puppini E., De Silvestri S. *Phys. Rev. B* **78**, 174422 (2008)
23. Ihama S., Sasaki Y., Naganuma H., Oogane M., Mizukami S., Ando Y. *J. Phys. D: Applied Physics* **49**, 035002 (2015)
24. Wietstruk M., Melnikov A., Stamm C., Kachel T., Pontius N., Sultan M., Gahl C., Weinelt M., Dürr H. A., Bovensiepen U. *Phys. Rev. Lett.* **106**, 127401 (2011)
25. Sultan M., Melnikov A., Bovensiepen U. *Phys. Status Solidi B* **248**, 2323 (2011)